A Novel Apolipoprotein E Antagonist Functionally Blocks Apolipoprotein E Interaction With N-terminal Amyloid Precursor Protein, Reduces β-Amyloid-Associated Pathology, and Improves Cognition

Darrell Sawmiller[*,1], **Ahsan Habib**[*,1], **Huayan Hou**[*,1], **Takashi Mori**[2], **Anran Fan**[1], **Jun Tian**[1], **Jin Zeng**[1], **Brian Giunta**[3], **Paul R. Sanberg**[4], **Mark P. Mattson**[5,6], and **Jun Tan**[1,#]

[1]Rashid Laboratory for Developmental Neurobiology, Silver Child Development Center, Department of Psychiatry & Behavioral Neurosciences, Morsani College of Medicine, University of South Florida, Tampa, Florida 33613, USA.

[2]Departments of Biomedical Sciences and Pathology, Saitama Medical Center and Saitama Medical University, Kawagoe, Saitama 350-8550, Japan.

[3]Neuroimmunology Laboratory, Department of Psychiatry & Behavioral Neurosciences, Morsani College of Medicine, University of South Florida, Tampa, Florida 33613, USA.

[4]Department of Neurosurgery & Brain Repair, Center for Aging and Brain Repair, Morsani College of Medicine, University of South Florida, Tampa, Florida 33613, USA.

[5]Laboratory of Neurosciences, National Institute on Aging Intramural Research Program, Baltimore, Maryland 21224, USA.

[6]Department of Neuroscience, Johns Hopkins University School of Medicine, Baltimore, Maryland 21224, USA.

Abstract

[#]Correspondence and requests for materials should be addressed to Jun Tan, Department of Psychiatry & Behavioral Neurosciences, Morsani College of Medicine, University of South Florida, Tampa, Florida, jtan@health.usf.edu.
[*]These authors contributed equally to this work.

BACKGROUND—The E4 isoform of apolipoprotein E (apoE4) is a major genetic risk factor for the development of sporadic Alzheimer's disease (AD) and its modification has been an intense focus for treatment of AD in recent years.

MEHTHODS—We investigated the binding of apoE, a peptide corresponding to its low density lipoprotein receptor (LDRL) binding domain (aa 133–152, ApoEp) and modified ApoEp to amyloid precursor protein (APP) and their effects on Aβ production in cultured cells. Having discovered a peptide which blocks the interaction of apoE with N-terminal APP, we investigated the effects of this peptide and ApoEp on AD-like pathology and behavioral impairment in 3XTg and 5XFAD transgenic mice.

RESULTS—ApoE and ApoEp, but not truncated apoE lacking the LDLR binding domain, physically interacted with N-terminal APP and thereby mediated Aβ production. Interestingly, the addition of six lysine residues to the N-terminal ApoEp (6KApoEp) directly inhibited apoE binding to N-terminal APP and markedly limited apoE- and ApoEp-mediated Aβ generation, presumably through decreasing APP cellular membrane trafficking and p44/42 mitogen-activated protein kinase phosphorylation. Moreover, while promoting apoE interaction with APP by ApoEp exacerbated Aβ and tau brain pathologies in 3XTg-AD mice, disrupting this interaction by 6KApoEp ameliorated cerebral Aβ and tau pathologies, neuronal apoptosis, synaptic loss, and hippocampal-dependent learning and memory impairment in 5XFAD mice without altering cholesterol, LDLR, and apoE expression levels.

CONCLUSIONS—These data suggest that disrupting apoE interaction with N-terminal APP may be a novel disease-modifying therapeutic strategy for AD.

INTRODUCTION

Afflicting as many as 47 million people worldwide, Alzheimer's disease (AD) is characterized by the accumulation of amyloid-β (Aβ) plaques and neurofibrillary tangles (NFTs) in the brain (1–4). Aβ is produced *via* β- and γ-secretase-mediated proteolysis of amyloid precursor protein (APP) (5,6), a type I transmembrane protein, which can then aggregate to form plaques. According to the amyloid hypothesis, overproduction of Aβ triggers neuronal apoptosis (7,8), inflammation (9, 10), oxidative stress (11,12), and tau phosphorylation and aggregation in intracellular neurofibrillary tangles (NFTs) (13). While inherited early-onset familial AD (FAD) results from mutations in *APP* or *presenilin (PS)* genes, in the more common late-onset sporadic AD (SAD) excess Aβ generation is enhanced by age-related factors, metabolic dysfunction, cardiovascular disease, and brain injury (14–16). In addition, the apoE4 isoform of apolipoprotein E (apoE4) has been found to be the major genetic risk factor for the development of SAD (17). Recently, since several therapeutic approaches targeting Aβ have failed, the relevance of Aβ in the AD pathogenesis has been questioned.

ApoE, a major component of chylomicron remnants and very-low, intermediate, and high-density peripheral-and brain-derived lipoproteins, plays an important role in receptor-mediated cholesterol endocytosis (18,19). The cause of the increased risk for AD associated with the presence of apoE4 may involve enhanced formation and reduced clearance of Aβ (20,21), the formation of neurotoxic apoE4 peptide fragments (22,23), abnormal tau phosphorylation, neuroinflammation, and neurodegeneration (24–27). Early studies utilizing yeast two-hybrid and immunoprecipitation suggested that the N-terminal APP can directly bind to apoE, thereby enhancing intracellular APP endocytosis and reducing sAPPα production (28). More recent study indicates that both glia-derived and recombinant apoE stimulates AP production in human neurons with a rank order of potency of apoE4 > apoE3 > apoE2, mediated by activation of a non-canonical mitogen activated protein kinase (MAPK) p44/p42 and enhanced transcription/translation of APP (29). These studies suggest that apoE directly binds to the N-terminal region of APP, thereby enhancing APP endocytosis and directing its processing from sAPPα to Ap. Recently, we further explored the binding of apoE to the N-terminal APP in Aβ production and generated a novel peptide antagonist of this interaction, which reduced Aβ production and pathology in AD mouse models. Taken together, our results suggest that disruption of apoE interaction with the N-terminal APP may be a novel disease-modifying therapeutic strategy for AD.

METHODS AND MATERIALS

Cell culture

CHO cells engineered to express human wild-type APP (CHO/APPwt) or Swedish mutant APP (CHO/APPswe) were cultured in 96 or 24 well plates at 4×10^4 or 2×10^5 cells/well, respectively, in Dulbecco's modified Eagle's medium (DMEM) with fetal bovine serum (FBS, 10%), 1 mM sodium pyruvate, and 100 U/mL of penicillin/streptomycin. In addition, SH-SY5Y cells transfected with APPswe and wild-type SH-SY5Y cells were cultured as previously described (30). Primary hN2™ human neurons were cultured in hN2™ human neuron culture media and primary HCN2 human neurons were cultured in DMEM with 4 mM L-glutamine adjusted to contain 1.5 g/L sodium bicarbonate, 4.5 g/L glucose, and FBS (10%).

Enzyme-linked immunosorbent assay, Western blotting, and immunoprecipitation

Aβ $_{1–40, 42}$ and sAPPα from cell cultures and brain homogenates were detected by Aβ and sAPPα enzyme-linked immunosorbent assay (ELISA) kits (IBL-America), strictly following the manufacturer's instructions (31,32). Western blotting (WB) analyses were performed as previously described (31,32). Immunoprecipitation (IP) was performed by first incubating conditioned media or cell lysates with appropriate antibodies and Protein-A/G Mag Sepharose beads (GE Healthcare Life Sciences, Pittsburgh, PA) overnight with gentle rocking at 4°C, followed by three washes with binding buffer (50 mM tris, 150 mM NaCl, pH 7.5) and analysis by WB. The effect of apoE4 and 6KApoEp on cell surface expression of APP, LDLR, and LRP1 was determined by biotinylation and avidin precipitation as described previously (33).

Real-Time PCR

Total RNA was extracted from CHO/APPwt cells after treatment with 6KApoEp using RNeasy Plus Mini Kit (Qiagen). The purity and concentration of RNA was quantified using Nanodrop 2000c spectrophotometer (Thermo Fisher Scientific). The quantification of target RNAs was performed in a total volume of 50 μL by real-time one-step RT-qPCR reactions (10 ng of RNA, 250 mM forward and reverse primers) using SYBR Green I in a IQ5 multi-color real-time PCR detection system (Bio-Rad), according to manufacturer's instructions. RNA primers were designed to selectively amplify and quantify human APP and LDLR and CHO cell β-actin (IDT) as indicated.

Cholesterol quantitation

For determination of CHO/APPwt cell associated cholesterol levels, cells were washed three times with ice-cold PBS, lysed by sonication in chloroform:isopropanol:IGEPAL CA-630 (7:11:0.1), and centrifuged. The organic phase was air dried at 50°C to remove chloroform and diluted 10-fold in the cholesterol assay buffer for the cholesterol determination by flourometric cholesterol quantitation kit according to manufacturer's instructions (MilliporeSigma).

Mice

All mice were housed and maintained in the Morsani College of Medicine Animal Facility at the University of South Florida (USF), and all experiments were conducted in compliance with protocols approved by the USF Institutional Animal Care and Use Committee. 5XFAD mice at 6 weeks of age (n = ten, five female/five male) were intraperitoneally (i.p.) treated with 6KApoEp (250 μg/kg in 50 μL PBS) or PBS (50 μL) daily for 12 weeks. 3XTg-AD mice at 9 months of age (n = six, three female/three male) were i.p. treated with ApoEp (250 μg/kg in 50 μL PBS) or PBS (50 μL) daily for 12 weeks. After 11-week treatment, 5XFAD mice were subjected to the Y Maze, fear conditioning, novel object recognition and open field behavioral testing as described previously (34,35).

After treatment and behavioral testing, all mice were anesthetized with 2–4 % isoflurane (Millipore Sigma), followed by collection of blood, euthanization by bilateral thoracotomy, transcardial perfusion with physiological saline containing heparin (10 U/mL, Millipore Sigma), and isolation of the brain for biochemical, immunohistochemical (IHC), and immunofluorescence (IF) analyses. Briefly, one hemisphere was frozen immediately in liquid nitrogen and stored at −80°C, followed by sonication in RIPA buffer (Cell Signaling Technology) containing protease inhibitor and phosphatase inhibitor cocktail (Thermo Fisher Scientific), centrifugation, and WB analysis of the supernatant. The other hemisphere was placed in 4% paraformaldehyde in PBS for cryostat sectioning. The 25-pm free-floating coronal sections were collected and stored in PBS with 100 mM sodium azide at 4°C for IHC and IF analyses.

IHC and IF

Brain sections from 5XFAD and 3XTg-AD mice were stained with biotin anti- Aβ $_{17–24}$ monoclonal antibody (4G8), VECTASTAIN *Elite* ABC Kit (Vector Laboratories, Burlingame, CA) and diaminobenzidine substrate, followed by quantitative image analysis

of Aβ burden, as described previously (31,32). In addition, brain coronal sections were analyzed by IHC staining with anti-acetylated tau (K^{174}, K^{274}) and anti-phosphorylated tau (Thr^{231}, Thr^{181}, Thr^{404}, and Ser^{202}/Thr^{205}) antibodies and IF staining with anti-β-tubulin III, anti-NeuN, anti-cleaved caspase-3, anti-synapsin I, anti-apoE, and anti-N-terminal APP antibodies. For thioflavin S staining, free floating brain tissues sections mounted on slides were washed in ddH_2O, stained in 1% filtered thioflavin S for 5 min and differentiated in 70% alcohol. For all cell culture and brain tissue staining analyses, images were taken by a BX60 microscope with an attached CCD camera system (DP-72, Olympus, Tokyo, Japan), or using an Olympus FV1000 laser scanning confocal microscope.

Statistical analysis

All data were normally distributed. Therefore, in instances of single mean comparisons, Levene's test for equality of variances followed by *t*-test for independent samples was used to assess significance. In instances of multiple mean comparisons, analysis of variance was used, followed by *post-hoc* comparison using Bonferonni's method. Alpha levels were set at 0.05 for all analyses. The statistical package for the social sciences release 23.0 (IBM SPSS) was used for all data analyses.

RESULTS

6KApoEp treatment markedly suppresses human recombinant and lipidated apoE-induced Aβ production

Previous findings suggest that apoE4 might exacerbate AD pathology, in part, by enhancing APP amyloidogenic processing (29). In addition, the N-terminal region of apoE (residues 133–152) is known to contain the apoE receptor binding domain, while structural modifications of apoE are known to mediate differential interaction of apoE isoforms with its receptor (21). In order to determine the specific region of apoE mediating Aβ production and further investigate the effects of structural modifications of apoE, we focused on the apoE LDLR binding domain and proximal structural modifications. As expected, an apoE peptide (ApoEp), consisting only of the LDLR binding domain of apoE (residues 133–152), markedly increased Aβ production in a concentration-dependent manner in CHO cells engineered to stably overexpress human wild-type APP (CHO/APPwt cells, Figure 1A, B and Supplement Figure 1A). Interestingly, while N-terminal addition of Flag-tag greatly enhanced the efficacy of ApoEp to increase $Aβ_{1–40, \ 42}$ levels, the addition of three lysine residues (3K) terminated this amyloidogenic effect (Figure 1A).

To test the hypothesis that the addition of N-terminal lysine residues might convert ApoEp to an apoE antagonist, we examined the effects of ApoEp containing 3, 6, 7, 8, or 9 lysines on apoE4-induced Aβ production. 3KApoEp moderately while 6 to 9KApoEp markedly and maximally reduced both basal and apoE4-induced Aβ production (Figure 1C and Supplement Figure 1B–D). In addition, 6KApoEp reduced apoE4-induced Aβ production in a concentration-dependent fashion, starting at 40 nM and with an IC50 of approximately 0.32 to 0.63 μM (Figure 1D, E and Supplement Figure 1C). This reduction was observed regardless of whether the cells were co-treated with 6KApoEp together with apoE4, pre-treated with 6KApoEp, or treated with apoE4 pre-incubated with 6KApoEp (Supplement

Figure 3). 6KApoEp also reduced Aβ production elicited by HDL-lipidated apoE4, human plasma-derived apoE3, and human astrocyte media-derived apoE in CHO/APPwt and SH-SY5Y human neuroblastoma cells as well as hN2™ and HCN2 human neurons (Figure 1F–H), confirming that 6KApoEp reduces natural apoE-mediated Aβ production.

6KApoEp reduces physical association of apoE with N-terminal APP

Previously, apoE was found to bind to the N-terminal APP, upstream of the Aβ region, and thereby enhances APP endocytosis and reduces sAPPα production (28). In order to confirm this physical association of apoE with N-terminal APP, CHO/APPwt cells were treated with ApoEp, 6KApoEp, 6K, apoE3, or apoE4 followed by immunoprecipitation (IP of apoE with anti-LDLR binding domain antibody (6H3B5). Total secreted APP in conditioned media and full length APP in cell lysates were then determined by WB analysis using anti-N-terminal (22C11) and anti-C-terminal APP antibodies (pC-APP), respectively. Alternatively, N-terminal APP was immunoprecipitated with anti-N-terminal APP41/66 antibody (pN-APP) followed by analysis of apoE, 6KApoEp, and ApoEp using anti-human apoE (mApoE) and 6H3B5 antibodies. ApoE, ApoEp, and 6KApoEp were co-immunoprecipitated with secreted APP in conditioned media and full length APP in cell lysates (Figure 2A, B and Supplement Figure 2A–C). In addition, ApoEp and 6KApoEp were co-localized with N-terminal APP in cultured CHO/APPwt cells, as determined by immunofluorescence (IF) staining with 6H3B5 and pN-APP antibodies (Figure 2C), respectively, confirming that N-terminal APP physically associates with apoE in vitro. ApoE was also co-immunoprecipated with N-terminal APP in homogenates prepared from brains of TgAPPwt mice, AD patients, and age-match controls, confirming that the physical association of apoE with N-terminal APP occurs in vivo (Figure 2D, E). Most interestingly, apoE was colocalized with cell surface APP more in brains from aged compared with young TgAPPwt mice, suggesting an age-associated increase in apoE-N-terminal APP interaction (Figure 2F). However, WB analysis showed no significant differences in total apoE and APP levels between young and aged TgAPPwt mouse brain homogenates (data not shown).

As in vitro confirmation of physical association of apoE with N-terminal APP, human recombinant sAPPβ (without Aβ domain), sAPPα, CHO/APPwt conditioned media-derived sAPPα (cmsAPPα), or APP N-terminal peptide (aa 31–60, APP31/60) was incubated with 6KApoEp, 6K, apoE3, or apoE4 followed by IP of apoE LDLR binding domain with 6H3B5 and WB analysis of sAPPα/β and APP31/60 (Figure 2G, H). Human recombinant sAPPα protein was also incubated with apoE4 in the absence or presence of 6KApoEp or 6K followed by IP with pN-APP and WB analysis of apoE and sAPPα (Figure 2I, J). Overall, sAPPα/β and APP31/60 were co-immunoprecipitated with 6KApoEp and apoE in vitro, confirming that 6KApoEp and apoE physically associates with N-terminal APP, and 6KApoEp reduced this association.

6KApoEp reduces Aβ production by blocking apoE interaction with N-terminal region of APP

Since 6KApoEp reduced apoE- and ApoEp-mediated Aβ production (Figure 1) as well as the physical association of apoE with N-terminal APP (Figure 2 and Supplement Figure 2), we wished to further investigate if apoE LDLR binding domain interaction with N-terminal

APP mediates Aβ production. Conditioned media collected from CHO/APPwt cells transiently coexpressing human wild-type apoE4 (CHO/APPwt/ApoEwt cells), truncated apoE4 lacking the LDLR binding domain (CHO/APPwt/ApoEtrun cells), or control vector (CHO/APPwt/Ctrl cells) were immunoprecipitated with anti-N-terminal APP antibody (pN-APP) followed by WB analysis of apoE and sAPPα. ApoEwt but not ApoEtrun was co-immunoprecipitated with sAPPα, confirming interaction of apoE with N-terminal APP *via* its LDLR binding domain (Figure 3A). As confirmation, ApoEwt but not ApoEtrun was co-localized with N-terminal APP, as determined by IF staining (Figure 3C). In addition, CHO/APPwt/ApoEwt cells produced markedly more Aβ than CHO/APPwt/ApoEtrun or CHO/APPwt/Ctrl cells. 6KApoEp reduced Aβ production in CHO/APPwt/ApoEwt cells and ApoEp enhanced Aβ production in CHO/APPwt/ApoEtrun cells, while conditioned media collected from CHO/APPwt/ApoEwt but not CHO/APPwt/ApoEtrun cells increased Aβ production in CHO/APPwt cells (Figure 3B). Thus, the apoE binding domain is required for apoE association with N-terminal APP and apoE-mediated Aβ production.

In order to confirm that apoE binding domain mediates Aβ production by interaction with the N-terminal region of APP, CHO/APPwt cells were treated with apoE3, apoE4, or ApoEp in the absence or presence of N-terminal APP (22C11) or apoE LDLR binding domain antibodies (6H3B5). Antibodies 22C11 and 6H3B5 reduced apoE3, apoE4, and ApoEp-mediated Aβ production in cultured cells in a dose-dependent fashion (Figure 4A and Supplement Figure 4). In addition, CHO/APPwt cells and CHO cells expressing truncated APP lacking the N-terminal E1 region (CHO/APPdE1 cells) were treated with 6KApoEp, ApoEp, apoE3, or apoE4 followed by analysis of Aβ production. CHO/APPdE1 cells produced markedly less Aβ production compared with CHO/APPwt cells after treatment with ApoEp, apoE3, or apoE4 (Figure 4B, *lower panel*). In contrast, CHO/APPwt and CHO/APPdE1 cells elicited similar spontaneous Aβ production in the absence of apoE and 6KApoEp reduced Aβ production elicited by CHO/APPwt but not CHO/APPdE1 cells. Therefore, apoE and ApoEp increases and 6KApoEp reduces Aβ production by binding to the N-terminal E1 region of APP, but this region of APP is not required for spontaneous Aβ release in the absence of apoE.

6KApoEp inhibits cell surface APP trafficking and p44/42 MAPK phosphorylation

Under physiological conditions, APP is known to be synthesized in the endoplasmic reticulum and trafficked *via* the trans-Golgi network to the plasma membrane where approximately 90% of it is cleaved by members of a disintegrin and metalloproteinase domain-containing protein (ADAM) (α-secretase), yielding a membrane-bound α-C-terminal APP fragment (α-CTF) and secreted sAPPα (36). The remaining unprocessed APP (~10%) can be cleaved at the plasma membrane or further trafficked back into the cell by endocytosis, followed by cleavage by β-site APP converting enzyme 1 (β-secretase, BACE1), yielding β-C-terminal fragment (β-CTF) and sAPPβ, and by γ-secretase, ultimately generating Aβ peptides which can then be secreted from the cell (37–39). Since α-secretase cuts APP within the Aβ region, increasing Aβ generation *via* the endocytic pathway precludes sAPPα production. We hypothesized that decreased Aβ generation by 6KApoEp might result from decreased membrane APP trafficking and subsequent amyloidogenic processing. To test this hypothesis, we investigated the effects of apoE4 and

6KApoEp on sAPPα and Aβ production into the media as well as β-CTF and total APP levels in the plasma membrane.

CHO/APPwt cells treated with apoE4 markedly increased Aβ and β-CTF levels, while reducing sAPPα levels, presumably by enhancing APP endocytosis (Figure 5A–C). Indeed, apoE4 enhanced Aβ and β-CTF levels much more in CHO/APPwt cells compared with CHO cells overexpressing APP with the Swedish mutation (CHO/APPswe cells), which is a better substrate for BACE1 and directly processed to Aβ prior to its trafficking to the cell surface (Supplement Figure 8). In contrast, 6KApoEp reduced both basal and more profoundly apoE4-induced production of Aβ, β-CTF, and sAPPα, without altering total APP levels, suggesting that 6KApoEp inhibits an early stage of APP processing, such as the initial trafficking of APP to the plasma membrane. As further confirmation, 6KApoEp reduced both basal and apoE4-mediated cell surface APP levels, as determined by WB, flow cytometry, and confocal microscopy, regardless of whether the cells were co-treated with 6KApoEp together with apoE4, pre-treated with 6KApoEp, or treated with apoE4 pre-incubated with 6KApoEp (Figure 5D–G and Supplement Figure 3B). 6KApoEp also reduced Aβ and β-CTF levels more in CHO/APPwt than in CHO/APPswe cells, consistent with reduction of APP trafficking to the cell surface (Supplement Figure 8). Notably, apoE4 and 6KApoEp, in the absence or presence of β- or γ-secretase inhibitors, did not alter cell surface protein levels of LDLR or LRP1 as well as mRNA levels of APP or LDLR, suggesting that apoE and 6KApoEp do not alter APP, LDLR and LRP1 expression or recycling (Figure 5D and Supplement Figures 9, 10).

Previously, apoE-mediated APP transcription/translation and Aβ production were found to be mediated by activation of a non-canonical p44/42 MAPK (29). In order to determine if apoE- and ApoEp-mediated APP trafficking and processing might also be mediated by this signaling pathway, we determined the effects of apoE, ApoEp, and 6KapoEp on p44/42 and p38 MAPK phosphorylation. While ApoEp, apoE3, and apoE4 activated both p44/42 and p38 MAPK phosphorylation, 6KApoEp only activated p38 MAPK phosphorylation and inhibited apoE-induced p44/42 phosphorylation (Figure 5H and Supplement Figure 5). Taken together, our findings suggest that ApoEp, apoE4, and 6KApoEp may have different effects on APP processing, with ApoEp and apoE4 enhancing and 6KApoEp reducing cell surface APP trafficking, APP endocytosis, and amyloidogenic processing, potentially mediated by differential activation of MAPK pathways.

6KApoEp reduces cerebral β-amyloid and tau pathologies, and memory impairment in AD mouse models

Since 6KApoEp inhibits apoE-APP receptor mediated Aβ generation, we examined if this apoE antagonist could reduce AD-like pathology in 5XFAD mice, known to develop extensive and aggressive β-amyloid neuropathology. In addition, we examined if mimicking the function of apoE by treatment with ApoEp could accelerate AD-like pathologies in 3XTg-AD mice, where Aβ seeding might play role in accelerating the progression of tau neuropathology. These mice were treated with ApoEp or 6KApoEp by intraperitoneal injection for 12 weeks and then euthanized, followed by analysis of cerebral Aβ and tau pathologies. Peripheral treatment of 3XTg-AD mice with ApoEp increased β-amyloid

plaques, as visualized by immunohistochemistry (IHC) with antibody 4G8, in comparison with mice treated with PBS as control (Figure 6A–C). Correspondingly, ApoEp increased levels of soluble $A\beta_{1-40, 42}$ and β-CTF, as determined by ELISA and WB analysis (Figure 6D, E), as well as levels of acetylated and phosphorylated tau, as evidenced by IHC and WB analyses (Figure 6F–K and Supplement Figure 6). In contrast, 6KApoEp treatment reduced β-amyloid plaques, Aβ, and β-CTF levels (Figure 7A–E and Supplement Figure 7) as well as phosphorylated and acetylated tau in 5XFAD mice (Figure 7F–K). In addition, 6KApoEp treatment enhanced synaptogenesis (presynaptic synapsin I and synaptophysin, and postsynaptic PSD95) and reduced neuronal apoptosis (cleaved caspase-3) (Figure 8).

In addition to determination of Aβ and tau pathologies, the effect of 6KApoEp on AD-like hippocampus-dependent learning and memory impairment was determined in 5XFAD mice utilizing the Y maze, fear conditioning, and novel object recognition tests. Untreated 5XFAD mice exhibited learning and memory impairment compared with non-transgenic control mice, as determined by reduced spontaneous alternation in the Y maze test, which was reversed by 6KApoEp treatment (Figure 9A). 6KApoEp treatment also reduced alternate arm entry returns in both 5XFAD and non-transgenic control mice (Figure 9B). Likewise, learning impairment in 5XFAD mice was exhibited by reduced freezing times during contextual and cued testing after fear conditioning (Figure 9E, F) and reduced ability to discriminate between familiar and novel objects (Figure 9G), which were all reversed upon treatment with 6KApoEp. Notably, 5XFAD mice exhibited some hyperactivity, as shown by enhanced total arm entries in the Y maze, which was reversed by 6KApoEp treatment (Figure 9C). However, 5XFAD and non-transgenic mice, whether untreated or treated with 6KApoEp, exhibited similar levels of anxiety since they spent similar amounts of time in central and peripheral zones of the open field (Figure 9H, I). Overall, these results confirm that while apoE accelerates Aβ and tau pathologies, antagonizing the effect of apoE by 6KApoEp reduces AD-like pathology, learning impairment, and hyperactivity in an AD mouse model.

DISCUSSION

In the present study, we explored the interaction of apoE with the N-terminal region of APP as a novel therapeutic target for AD. Based on previous studies that suggest that this interaction may enhance Aβ production (28,29), we initially focused on the apoE LDLR binding domain (residues 133–152, ApoEp). Like apoE, we found that ApoEp also interacts with N-terminal APP and dose-dependently increases Aβ production (Figures 1, 2). Antibodies against the N-terminal region of APP or the LDLR binding domain of apoE and truncation of the N-terminal domain of APP reduced apoE-mediated Aβ production (Figures 3, 4). Thus, the apoE LDLR binding domain increases Aβ production by interacting with the N-terminal APP. Moreover, 6KApoEp, addition of lysine residues to the N-terminal apoE inhibited apoE- and ApoEp- mediated Aβ production, presumably through decreasing apoE-N-terminal APP interaction, APP cellular membrane trafficking and p44/42 MAPK phosphorylation (Figure 5 and Figure 10).

Based on our findings in vitro, we further investigated the potential of 6KApoEp, as a therapeutic agent for the treatment of AD-like pathology in AD mouse models. While

ApoEp enhanced A$\beta_{1-40, 42}$ levels and β-amyloid plaque as well as acetylated and phosphorylated tau in 3XTg-AD mice (Figure 6), 6KApoEp reduced AD-like pathology in 5XFAD mice, reducing β-amyloid plaques, acetylated and phosphorylated tau, apoptosis, and neuroinflammation, while enhancing synaptogenesis and improving hippocampus-dependent learning and memory functions (Figures 7–9 and Supplement Figure 11). In addition, 6KApoEp presumably elicited its therapeutic effects without altering cholesterol homeostasis (Supplement Figure 12). Taken together, these findings point to the potential of 6KApoEp as a via ble therapeutic agent for the treatment of AD pathology and behavioral impairment.

Our study suggests that 6KApoEp reduces AD-like pathology by interfering the physical interaction of apoE with N-terminal APP. Based on our findings, we suggest that apoE might have a dual function in the brain, (1) mediating cholesterol transport into the neuron and thereby promoting neuronal proliferation, differentiation, and health (18,19) and (2) binding to N-terminal APP and thereby promoting APP amyloidogenic proteolysis and resultant AD-like pathology (28,29). While the cholesterol transporting role of apoE may function well in the young and healthy brain, the APP proteolytic role of apoE might be expected to be a function of aging and disease. This hypothesis is also based on recent findings that APP has a receptor function like other type 1 transmembrane receptors, which either mediates axon guidance, synaptogenesis, and growth factor signaling or AD pathogenesis, depending on the environment (40–44). For example, over-stimulation of APP by apoE might lead to over-activation of Go protein and APP intercellular domain (AICD), which can be pathogenic. In addition, other factors such as apoE lipidation, glycosylation, and oxidation could play a role in determining how apoE functions. Clearly, the interaction of apoE with N-terminal APP as a therapeutic target for AD should be further explored.

Lastly, our novel apoE antagonist 6KApoEp might be expected to be particularly beneficial for AD patients who are apoE4 carriers as well as those carrying apoE3. ApoE3 and apoE4 have a much stronger binding affinity to its receptors compared with apoE2 (45) and individuals carrying the lower affinity apoE2 are protected against AD and have much less accumulation of β-amyloid pathology in the brain as they age (46,47). Clinically, older apoE2 carriers display superior verbal learning abilities, improved recall memory, faster processing of information, and better test performance (47). 6KApoEp may specifically counteract the adverse effects of apoE4 by dampening its binding to receptors. A better understanding for the role of apoE isoforms in neuroplasticity and AD as well as their interaction with N-terminal APP and molecular mechanisms may reveal novel approaches for extending brain health span.

Supplementary Material

Refer to Web version on PubMed Central for supplementary material.

ACKNOWLEDGEMENTS

REFERENCES

1. Glenner GG, Wong CW (1984): Alzheimer's disease: initial report of the purification and characterization of a novel cerebrovascular amyloid protein. Biochem Biophys Res Commun 120:885–890. [PubMed: 6375662]

2. Grundke-Iqbal I, Iqbal K, Tung YC, Quinlan M, Wisniewski HM, Binder LI (1986): Abnormal phosphorylation of the microtubule-associated protein tau (tau) in Alzheimer cytoskeletal pathology. Proc Natl Acad Sci U S A 83:4913–4917. [PubMed: 3088567]

3. Selkoe DJ (2001): Alzheimer's disease: genes, proteins, and therapy. Physiol Rev 81:741–766. [PubMed: 11274343]

4. Hardy J, Selkoe DJ (2002): The amyloid hypothesis of Alzheimer's disease: progress and problems on the road to therapeutics. Science 297:353–356. [PubMed: 12130773]

5. Schenk DB, Rydel RE, May P, Little S, Panetta J, Lieberburg I, et al. (1995): Therapeutic approaches related to amyloid-β peptide and Alzheimer's disease. J Med Chem 38:4141–4154. [PubMed: 7473539]

6. Selkoe DJ, Yamazaki T, Citron M, Podlisny MB, Koo EH, Teplow DB, et al. (1996): The role of APP processing and trafficking pathways in the formation of amyloid β-protein. Ann N Y Acad Sci 777:57–64. [PubMed: 8624127]

7. LaFerla FM, Tinkle BT, Bieberich CJ, Haudenschild CC, Jay G (1995): The Alzheimer's Aβ peptide induces neurodegeneration and apoptotic cell death in transgenic mice. Nat Genet 9:21–30. [PubMed: 7704018]

8. Loo DT, Copani A, Pike CJ, Whittemore ER, Walencewicz AJ, Cotman CW (1993): Apoptosis is induced by β-amyloid in cultured central nervous system neurons. Proc Natl Acad Sci U S A 90:7951–7955. [PubMed: 8367446]

9. Bradt BM, Kolb WP, Cooper NR (1998): Complement-dependent proinflammatory properties of the Alzheimer's disease β-peptide. J Exp Med 188:431–438. [PubMed: 9687521]

10. Suo Z, Tan J, Placzek A, Crawford F, Fang C, Mullan M (1998): Alzheimer's β-amyloid peptides induce inflammatory cascade in human vascular cells: the roles of cytokines and CD40. Brain Res 807:110–117. [PubMed: 9757011]

11. Hensley K, Carney JM, Mattson MP, Aksenova M, Harris M, Wu JF, et al. (1994): A model for β-amyloid aggregation and neurotoxicity based on free radical generation by the peptide: relevance to Alzheimer disease. Proc Natl Acad Sci U S A 91:3270–3274. [PubMed: 8159737]

12. Murakami K, Irie K, Ohigashi H, Hara H, Nagao M, Shimizu T, et al. (2005): Formation and stabilization model of the 42-mer Aβ radical: implications for the long-lasting oxidative stress in Alzheimer's disease. J Am Chem Soc 127:15168–15174. [PubMed: 16248658]

13. Lee VM, Trojanowski JQ (2006): Progress from Alzheimer's tangles to pathological tau points towards more effective therapies now. J Alzheimers Dis 9:257–262. [PubMed: 16914864]

14. Rocca WA, Amaducci LA, Schoenberg BS (1986): Epidemiology of clinically diagnosed Alzheimer's disease. Ann Neurol 19:415–424. [PubMed: 3717905]

15. Elias MF, Elias PK, Sullivan LM, Wolf PA, D'Agostino RB (2003): Lower cognitive function in the presence of obesity and hypertension: the Framingham heart study. Int J Obes Relat Metab Disord 27:260–268. [PubMed: 12587008]

16. Kapogiannis D, Mattson MP (2011): Disrupted energy metabolism and neuronal circuit dysfunction in cognitive impairment and Alzheimer's disease. Lancet Neurol 10:187–198. [PubMed: 21147038]

17. Eisenstein M (2011): Genetics: finding risk factors. Nature 475:S20–22. [PubMed: 21760580]

18. Mahley RW (1988): Apolipoprotein E: cholesterol transport protein with expanding role in cell biology. Science 240:622–630. [PubMed: 3283935]

19. Mahley RW, Weisgraber KH, Huang Y (2009): Apolipoprotein E: structure determines function, from atherosclerosis to Alzheimer's disease to AIDS. J Lipid Res 50 Suppl:S183–188. [PubMed: 19106071]

20. Castellano JM, Kim J, Stewart FR, Jiang H, DeMattos RB, Patterson BW, et al. (2011): Human apoE isoforms differentially regulate brain amyloid-β peptide clearance. Sci Transl Med 3:89ra57.

21. Ye S, Huang Y, Mullendorff K, Dong L, Giedt G, Meng EC, et al. (2005): Apolipoprotein (apo) E4 enhances amyloid β peptide production in cultured neuronal cells: apoE structure as a potential therapeutic target. Proc Natl Acad Sci U S A 102:18700–18705. [PubMed: 16344478]

22. Harris FM, Brecht WJ, Xu Q, Tesseur I, Kekonius L, Wyss-Coray T, et al. (2003): Carboxyl-terminal-truncated apolipoprotein E4 causes Alzheimer's disease-like neurodegeneration and behavioral deficits in transgenic mice. Proc Natl Acad Sci U S A 100:10966–10971. [PubMed: 12939405]

23. Brecht WJ, Harris FM, Chang S, Tesseur I, Yu GQ, Xu Q, et al. (2004): Neuron-specific apolipoprotein E4 proteolysis is associated with increased tau phosphorylation in brains of transgenic mice. J Neurosci 24:2527–2534. [PubMed: 15014128]

24. Wang C, Najm R, Xu Q, Jeong DE, Walker D, Balestra ME, et al. (2018): Gain of toxic apolipoprotein E4 effects in human iPSC-derived neurons is ameliorated by a small-molecule structure corrector. Nat Med 24:647–657. [PubMed: 29632371]

25. Shi Y, Yamada K, Liddelow SA, Smith ST, Zhao L, Luo W, et al. (2017): ApoE4 markedly exacerbates tau-mediated neurodegeneration in a mouse model of tauopathy. Nature 549:523–527. [PubMed: 28959956]

26. Uddin MS, Kabir MT, Al Mamun A, Abdel-Daim MM, Barreto GE, Ashraf GM (2018): APOE and Alzheimer's Disease: Evidence Mounts that Targeting APOE4 may Combat Alzheimer's Pathogenesis. Mol Neurobiol (Epub ahead of print).

27. Zhao N, Liu CC, Qiao W, Bu G (2018): Apolipoprotein E, Receptors, and Modulation of Alzheimer's Disease. Biol Psychiatry 83:347–357. [PubMed: 28434655]

28. Hass S, Fresser F, Kochl S, Beyreuther K, Utermann G, Baier G (1998): Physical interaction of ApoE with amyloid precursor protein independent of the amyloid Aβ region in vitro. J Biol Chem 273:13892–13897. [PubMed: 9593736]

29. Huang YA, Zhou B, Wernig M, Sudhof TC (2017): ApoE2, ApoE3, and ApoE4 Differentially Stimulate APP Transcription and Aβ Secretion. Cell 168:427–441 e421. [PubMed: 28111074]

30. Rezai-Zadeh K, Shytle D, Sun N, Mori T, Hou H, Jeanniton D, et al. (2005): Green tea epigallocatechin-3-gallate (EGCG) modulates amyloid precursor protein cleavage and reduces cerebral amyloidosis in Alzheimer transgenic mice. J Neurosci 25:8807–8814. [PubMed: 16177050]

31. Obregon D, Hou HY, Deng J, Giunta B, Tian J, Darlington D, et al. (2012): Soluble amyloid precursor protein-a modulates β-secretase activity and amyloid-β generation. Nat Commun 3:777. [PubMed: 22491325]

32. Zhu Y, Hou H, Rezai-Zadeh K, Giunta B, Ruscin A, Gemma C, et al. (2011): CD45 deficiency drives amyloid-β peptide oligomers and neuronal loss in Alzheimer's disease mice. J Neurosci 31:1355–1365. [PubMed: 21273420]

33. Li S, Deng J, Hou H, Tian J, Giunta B, Wang Y, et al. (2014): Specific antibody binding to the APP672–699 region shifts APP processing from α- to β-cleavage. Cell Death Dis 5:e1374. [PubMed: 25118934]

34. Sawmiller D, Li S, Mori T, Habib A, Rongo D, Delic V, et al. (2017): Beneficial effects of a pyrroloquinolinequinone-containing dietary formulation on motor deficiency, cognitive decline and mitochondrial dysfunction in a mouse model of Alzheimer's disease. Heliyon 3:e00279. [PubMed: 28413833]

35. Sawmiller D, Habib A, Li S, Darlington D, Hou H, Tian J, et al. (2016): Diosmin reduces cerebral Aß levels, tau hyperphosphorylation, neuroinflammation, and cognitive impairment in the 3xTg-AD mice. J Neuroimmunol 299:98–106. [PubMed: 27725131]

36. Haass C, Selkoe DJ (1993): Cellular processing of beta-amyloid precursor protein and the genesis of amyloid β-peptide. Cell 75:1039–1042. [PubMed: 8261505]

37. Habib A, Sawmiller D, Tan J (2017): Restoring Soluble Amyloid Precursor Protein α Functions as a Potential Treatment for Alzheimer's Disease. J Neurosci Res 95:973–991. [PubMed: 27531392]

38. Eggert S, Thomas C, Kins S, Hermey G (2018): Trafficking in Alzheimer's Disease: Modulation of APP Transport and Processing by the Transmembrane Proteins LRP1, SorLA, SorCS1c, Sortilin, and Calsyntenin. Mol Neurobiol 55:5809–5829. [PubMed: 29079999]

39. Zhang X, Song W (2013): The role of APP and BACE1 trafficking in APP processing and amyloid-β generation. Alzheimers Res Ther 5:46. [PubMed: 24103387]

40. Bukhari H, Glotzbach A, Kolbe K, Leonhardt G, Loosse C, Müller T (2017): Small things matter: Implications of APP intracellular domain AICD nuclear signaling in the progression and pathogenesis of Alzheimer's disease. Prog Neurobiol 156:189–213. [PubMed: 28587768]

41. Copenhaver PF, Kögel D (2017): Role of APP Interactions with Heterotrimeric G Proteins: Physiological Functions and Pathological Consequences. Front Mol Neurosci 10:3. [PubMed: 28197070]

42. Dawkins E, Small DH (2014): Insights into the physiological function of the β-amyloid precursor protein: beyond Alzheimer's disease. J Neurochem 129:756–769. [PubMed: 24517464]

43. Deyts C, Thinakaran G, Parent AT (2016): APP Receptor? To Be or Not To Be. Trends Pharmacol Sci 37:390–411. [PubMed: 26837733]

44. Sosa LJ, Caceres A, Dupraz S, Oksdath M, Quiroga S, Lorenzo A (2017): The physiological role of the amyloid precursor protein as an adhesion molecule in the developing nervous system. J Neurochem 143:11–29. [PubMed: 28677143]

45. Bu G (2009): Apolipoprotein E and its receptors in Alzheimer's disease: pathways, pathogenesis and therapy. Nat Rev Neurosci 10:333–344. [PubMed: 19339974]

46. Benjamin R, Leake A, McArthur FK, Ince PG, Candy JM, Edwardson JA, et al. (1994): Protective effect of apoE ε2 in Alzheimer's disease. Lancet 344:473.

47. Suri S, Heise V, Trachtenberg AJ, Mackay CE (2013): The forgotten APOE allele: a review of the evidence and suggested mechanisms for the protective effect of APOE ε2. Neurosci Biobehav Rev 37:2878–2886. [PubMed: 24183852]

48. Tokuda T, Calero M, Matsubara E, Vidal R, Kumar A, Permanne B, et al. (2000): Lipidation of apolipoprotein E influences its isoform-specific interaction with Alzheimer's amyloid β peptides. Biochem J 348 Pt 2:359–365. [PubMed: 10816430]

49. Krul ES, Tang J (1992): Secretion of apolipoprotein E by an astrocytoma cell line. J Neurosci Res 32:227–238. [PubMed: 1404494]
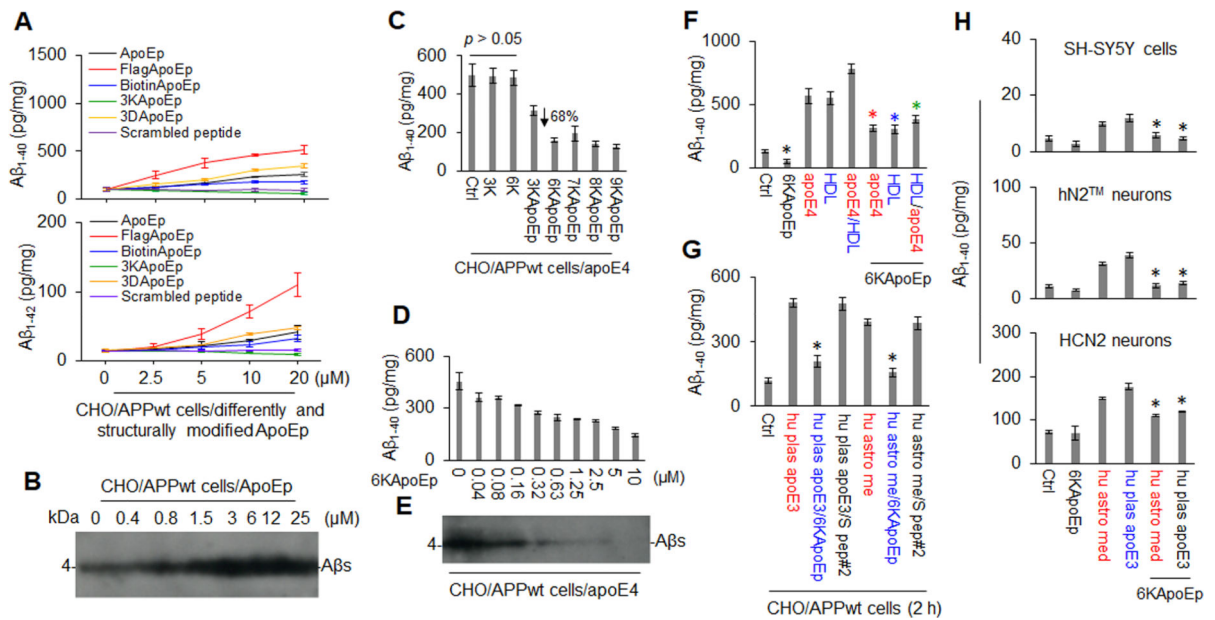
Figure 1. 6KApoEp markedly inhibits human recombinant and lipidated apoE-mediated Aβ production.

CHO/APPwt cells were treated with apoE LDLR binding domain peptide (aa 133–152, ApoEp), FlagApoEp, BiotinApoEp, 3K (lysine) ApoEp, 3D (aspartate) ApoEp, or scrambled peptide at 0 to 25 μM, followed after 2 h by analysis of Aβ levels in conditioned media by Aβ ELISA (**A**) and after 16 h by analysis of Aβ in cell lysates by Western blot (WB) using 82E1 antibody (**B**). In addition, CHO/APPwt cells were treated with PBS (Ctrl) or 3K (3 lysines), 6K, 3KApoEp, 6KApoEp, 7KApoEp, 8KApoEp, or 9KApoEp at 10 μM, or 6KApoEp at 0 to 10 μM, for 15 min, followed by the addition of human recombinant apoE4 (apoE4) at 10 μg/mL and then Aβ ELISA (2 h, **C, D**) and WB (16 h, **E**). CHO/APPwt cells, SH-SY5Y neuroblastoma cells, hN2™ human neurons and HCN2 cortical neurons were also treated with apoE4, human plasma derived-HDL (HDL) or human plasma-derived apoE3 (hu plas apoE3) at 10 μg/mL, apoE4 pre-incubated with HDL for 1 h at 37°C (apoE4/HDL), or human astrocyte-derived media (hu astro med) at 1:4 dilution in the absence or presence of 6KApoEp or scrambled peptide (S pep#2) at 10 μM, followed by Aβ ELISA (**F-H**). Pre-incubating with HDL has been previously reported to lipidate apoE (48). Hu astro med was obtained from human astrocytes (CCF-STTG1/ATCC® CRL-1718™) as described previously (49). ELISA results representative of three independent experiments with each condition duplicated and presented as the mean (± s.d.) of Aβ (pg/mg of total intracellular protein). Asterisk indicates $p < 0.05$ for ApoEp-, FlagApoEp-, BiotinApoEp- or 3DApoEp-mediated Aβ production, compared with scramble peptide (#1)- or 3KApoEp, as determined by one-way ANOVA (**A**) and for apoE4-, hu plas apoE3-, or hu astro media-mediated Aβ production in the presence compared with the absence of 6KApoEp as determined by t test (**F-H**).
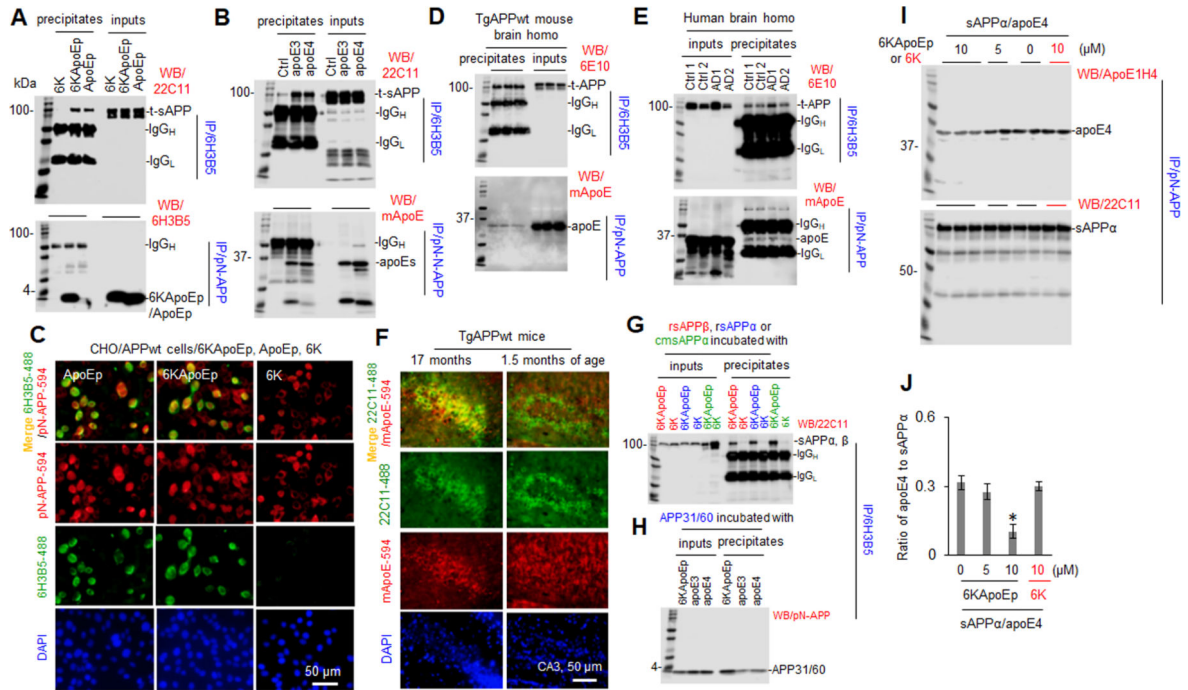
Figure 2. 6KApoEp physically interacts with N-terminal APP.

CHO/APPwt cells were treated with 6KApoEp, ApoEp, or 6K at 10 μM (**A**), apoE3 or 4 at 10 μg/mL, or PBS control (Ctrl, **B**) for 2 h followed by immunoprecipitation (IP) of the conditioned media with mouse monoclonal anti-apoE LDL binding domain antibody (6H3B5) or rabbit polyclonal anti-N-terminal APP41/66 antibody (pN-APP). Total secreted APP (t-sAPP), 6KApoEp, ApoEp, apoE3, and apoE4 4 in total conditioned media (inputs) and immunoprecipitates (precipitates) was then determined by WB using mouse anti-N-terminal APP antibody (22C11), 6H3B5, and rabbit anti-human apoE antibody (mApoE) (**A, B**), respectively. CHO/APPwt cells were also plated at 8 well-chambers at 1×10^5/well for 24 h, treated with 6K, ApoEp, or 6KApoEp at 10 μM for 2 h, fixed in 4% paraformaldehyde solution and stained with 6H3B5 and pN-APP (**C**). Alexa Fluor 488 goat anti-mouse IgG was used to detect ApoEp and 6KApoEp (green), while Alexa Fluor 594 donkey anti-rabbit IgG was used to detect N-terminal APP (red). DAPI costaining showed nuclear DNA. Brain tissue homogenates prepared from three TgAPPwt mice (two female/one male), two AD patients (AD1/male, AD2/female) and two normal age-matched control cortices (Ctrl1/male, Ctrl2/female) were IP with 6H3B5 or pN-APP and t-APP and apoE were determined by WB analysis using 6E10 and mApoE, respectively (**D, E**). Brain tissue sections from aged and young TgAPPwt mice (n = two for each group, one female/one male) were also stained with 22C11 and mApoE at 4°C overnight, followed by staining with Alexa Fluor 488 goat anti-mouse IgG to detect cell surface APP (green) and Alexa Fluor 594 donkey anti-rabbit IgG to detect apoE (red, **F**). As in vitro confirmation, human recombinant sAPPβ (rsAPPβ, without Aβ domain), rsAPPα, CHO/APPwt cell conditioned media-derived sAPPα (cmsAPPα), or APP N-terminal peptide (aa 31–60, APP31/60) at 100 nM was incubated with 6KApoEp, 6K, apoE3, or apoE4 at 100 nM, at 37°C for 1 h followed by IP with 6H3B5. sAPPα/β and APP31/60 in total (inputs) and immunoprecipitates were determined by WB analysis using 22C11and pN-APP, respectively (**G, H**). In addition, human sAPPα protein at 100 nM was

also incubated with apoE4 protein at 100 nM in the absence or presence of 6KApoEp or 6K at 5 or 10 μM for 1 h at 37°C, followed by IP with pN-APP and determination of apoE4 and sAPPα in precipitates by WB analysis using ApoE1H4 and 22C11, respectively (**I**). Band density ratios of apoE4 to total sAPPα was determined by densitometry analysis (**J**). The results shown in **J** panel are representative of two independent experiments with each condition duplicated. Asterisk indicates $p < 0.05$ compared with the controls as determined by *t*-test. Overall, 6KApoEp, ApoEp, apoE3, and apoE4, but not 6K, were immunoprecipitated and localized with N-terminal APP in vitro and in vivo. ApoE was co-localized with N-terminal APP more in aged compared with young TgAPPwt mouse brains. 6KApoEp, but not 6K, reduced co-immunoprecipitation of sAPPα with apoE4. AD patient and age-matched control cortices provided by Banner Sun Health Research Institute (Sun City, AZ). The results shown in **A-D** panels are representative of two to three independent experiments.
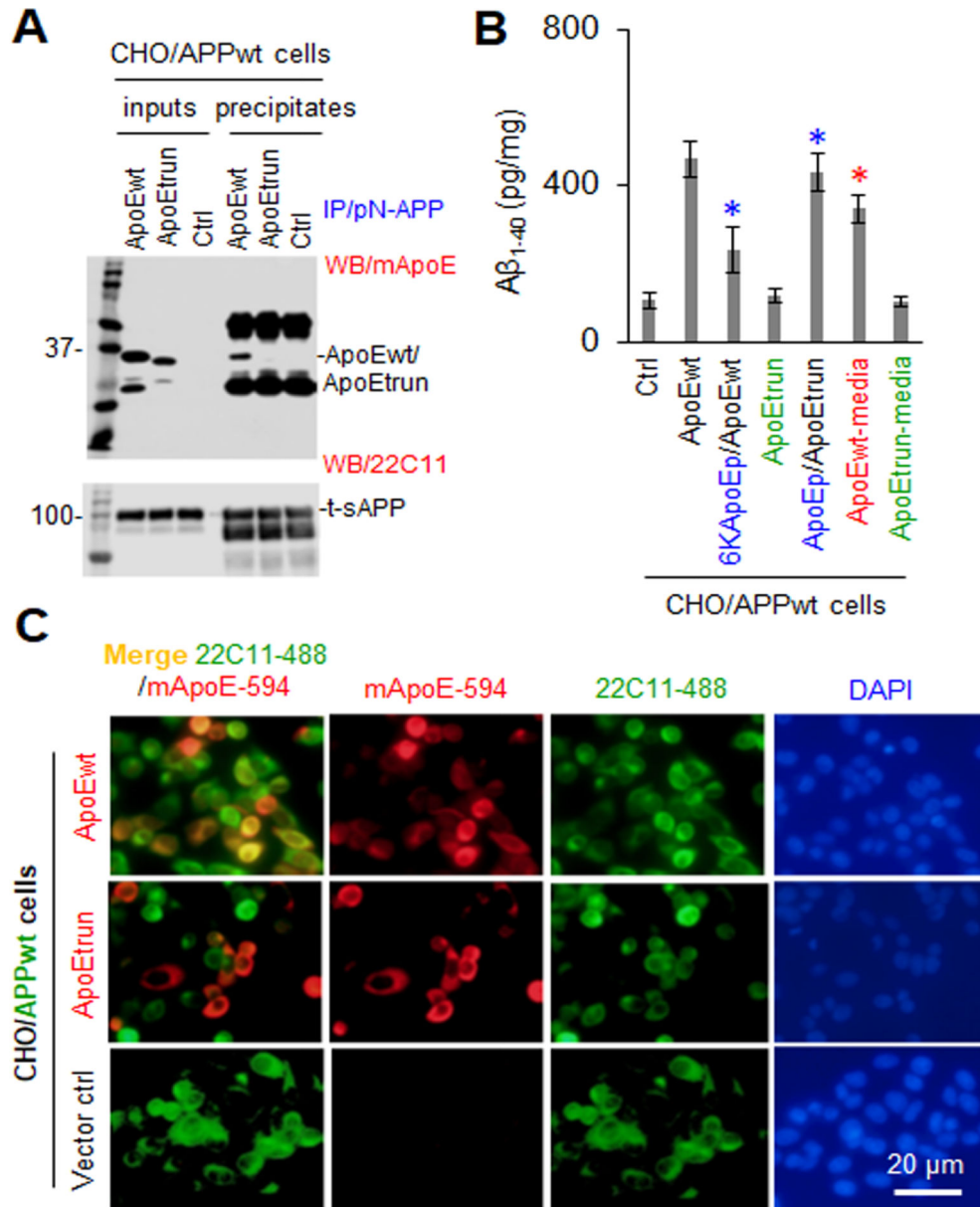
Figure 3. Truncated apoE lacking the LDLR binding domain failed to promote Aβ production in CHO/APPwt cells.

Conditioned media collected from CHO/APPwt cells co-transiently expressing human wild-type apoE4 (CHO/APPwt/ApoEwt), truncated apoE4 lacking the LDLR binding domain (CHO/APPwt/ApoEtrun), or control vector (CHO/APPwt/Ctrl) were immunoprecipitated with pN-APP and then apoE and sAPPα in total conditioned media (inputs) and immunoprecipitates were determined by WB analysis using mApoE and 22C11, respectively (**A**). In addition, CHO/APPwt/ApoEwt, CHO/APPwt/ApoEtrun, and CHO/APPwt/Ctrl cells were cultured on 24 well plates at 1×10^5/well overnight and then treated with 6KApoEp or ApoEp at 10 μM, and CHO/APPwt/Ctrl cells were treated with conditioned media collected from CHO/APPwt/ApoEwt or CHO/APPwt/ApoEtrun cells, for 2 h followed by Aβ ELISA (**B**). Furthermore, CHO/APPwt/ApoEwt, CHO/APPwt/ApoEtrun, or CHO/APPwt/Ctrl cells

were also plated at 8 well-chambers at 1×10^5/well for 24 h, fixed in 4% paraformaldehyde solution and stained with mouse monoclonal anti-N-terminal APP (22C11) and rabbit monoclonal anti-apoE antibodies (mApoE, **C**). Alexa Fluor 488 goat anti-mouse IgG was used to detect cell surface APP (green), while Alexa Fluor 594 donkey anti-rabbit IgG was used to detect apoE (red). ApoEwt but not ApoEtrun was co-immunoprecipitated (**A**) and co-localized with cell surface APP (**C,** *left panels merged*) and enhanced Aβ production (**B**), indicating that the LDLR binding domain is necessary for apoE interaction with the N-terminal APP. Notably, 6KApoEp markedly reduced Aβ production in CHO/APPwt/ApoEwt cells, while ApoEp significantly restored Aβ production in CHO/APPwt/ApoEtrun cells (**B**). ELISA results are representative of three independent experiments with each condition duplicated and presented as the mean (± s.d.) of Aβ (pg/mg total intracellular protein). Asterisks indicates $p < 0.05$ for Aβ production in the presence compared with corresponding absence of 6KApoEp or ApoEp or in the presence of CHO/APPwt/ApoEwt compared with CHO/APPwt/ApoEtrun media as determined by *t* test.
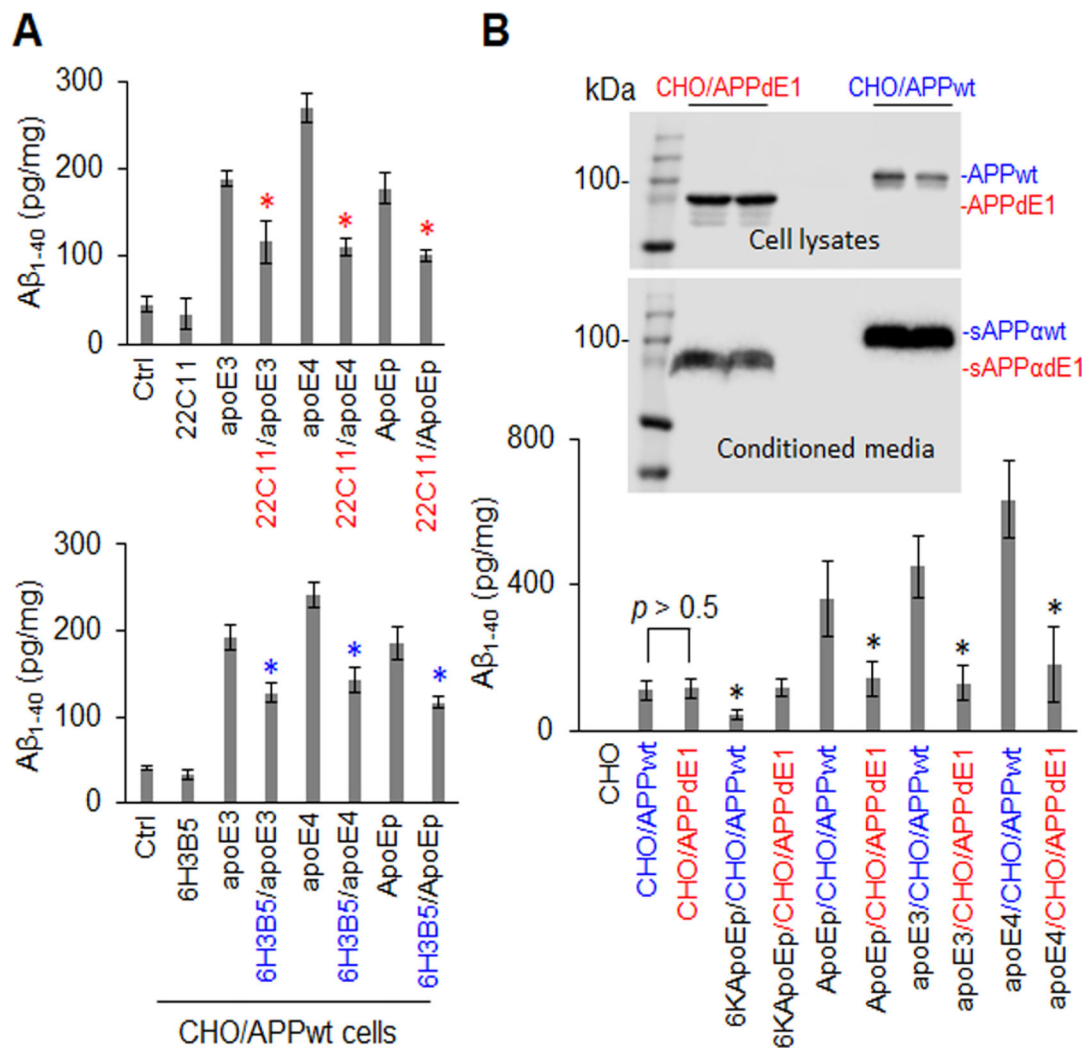
Figure 4. ApoE-promoted Aβ production was significantly attenuated by specific antibodies against the apoE LDLR binding domain or the N-terminal APP or by expression of N-terminally truncated APP.

CHO/APPwt cells were treated with apoE3 or apoE4 at 10 mg/mL or ApoEp at 5 μM in the absence or presence of anti-N-terminal APP (22C11) or anti-apoE LDLR binding domain antibody (6H3B5) at 10 μg/mL for 2 h followed by Aβ ELISA (**a**). CHO cells were also transfected with pCMV6 APP695 or pCMV6 E1 depleted APP695, yielding cells expressing wild-type APP695 (CHO/APPwt) or truncated APP695 lacking the N-terminal E1 region (CHO/APPdE1). After 24 h, the cells were treated with 6KApoEp or ApoEp at 10 μM, or apoE3 or apoE4 at 10 μg/mL, for 3 h followed by Aβ ELISA (**B**, *lower panel*). APPwt/dE1 in cell lysates and sAPPαwt/dE1 in conditioned media derived from the transfected CHO cells were determined by WB analysis using 6E10 (**B**, *top panels*). ApoE3-, apoE4-, and ApoEp-mediated Aβ production were markedly reduced by 22C11, 6H3B5, and truncation of the dE1 region of APP, indicating that apoE-mediated Aβ production is mediated by interaction of apoE LDLR binding domain with N-terminal APP. Isotype-matched control IgG failed to reduce apoE3, apoE4, or ApoEp-mediated Aβ production (data not shown). ELISA results are representative of three independent experiments with each condition

triplicated and presented as the mean (± s.d.) of Aβ (pg/mg of total intracellular protein). Asterisk indicates $p < 0.05$ compared with the corresponding absence of 22C11 or 6H3B5, or corresponding CHO/APPwt cells as determined by one-way ANOVA.
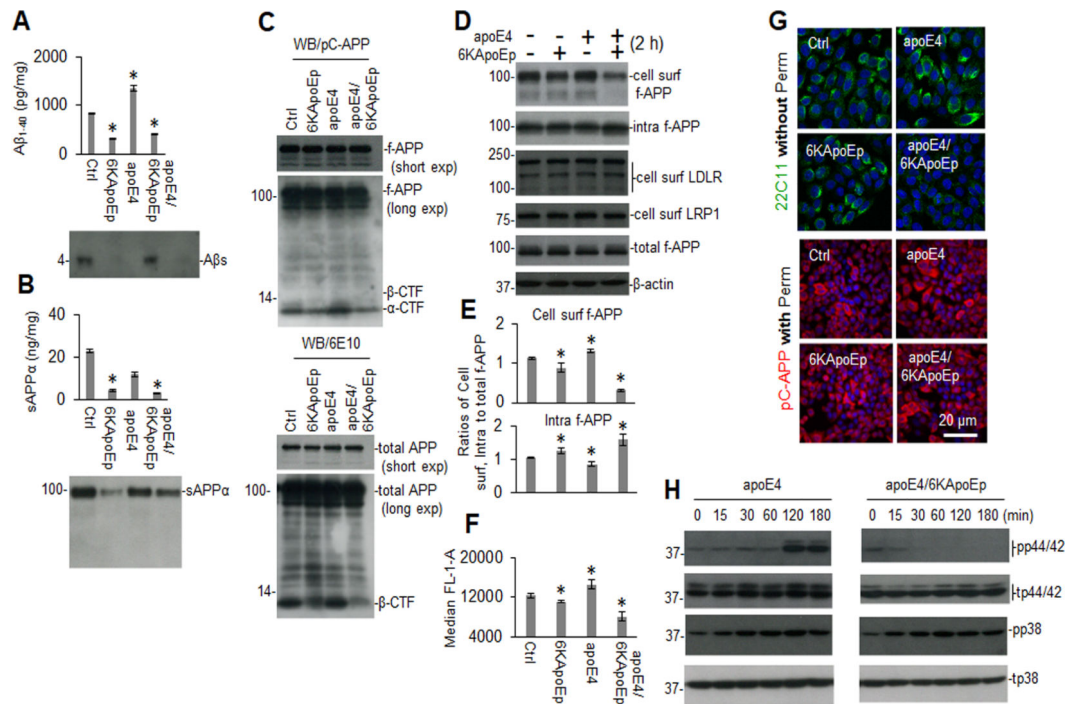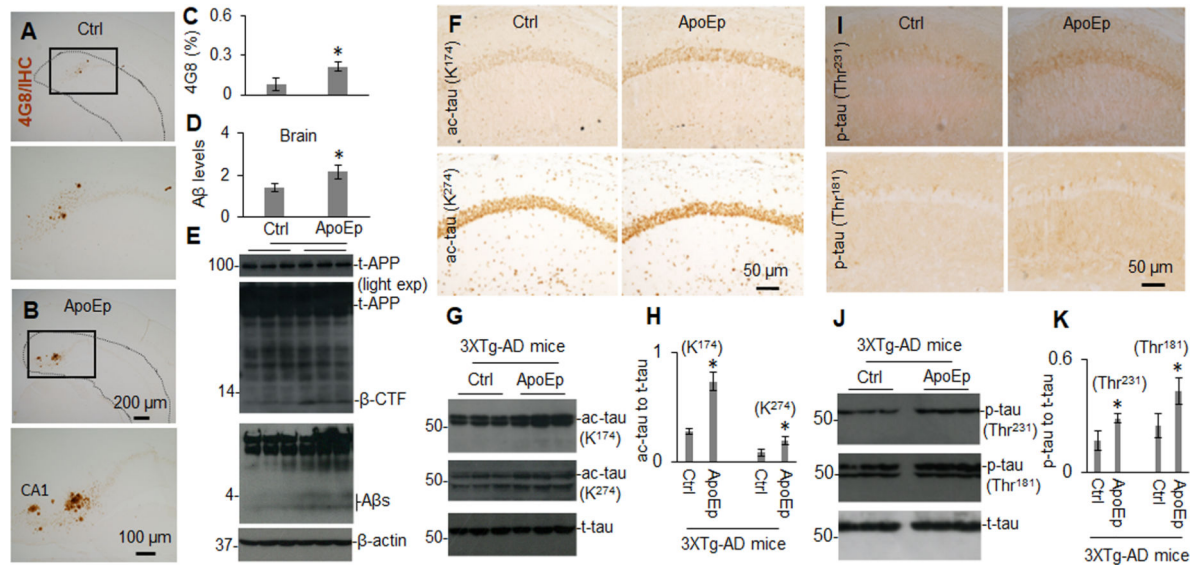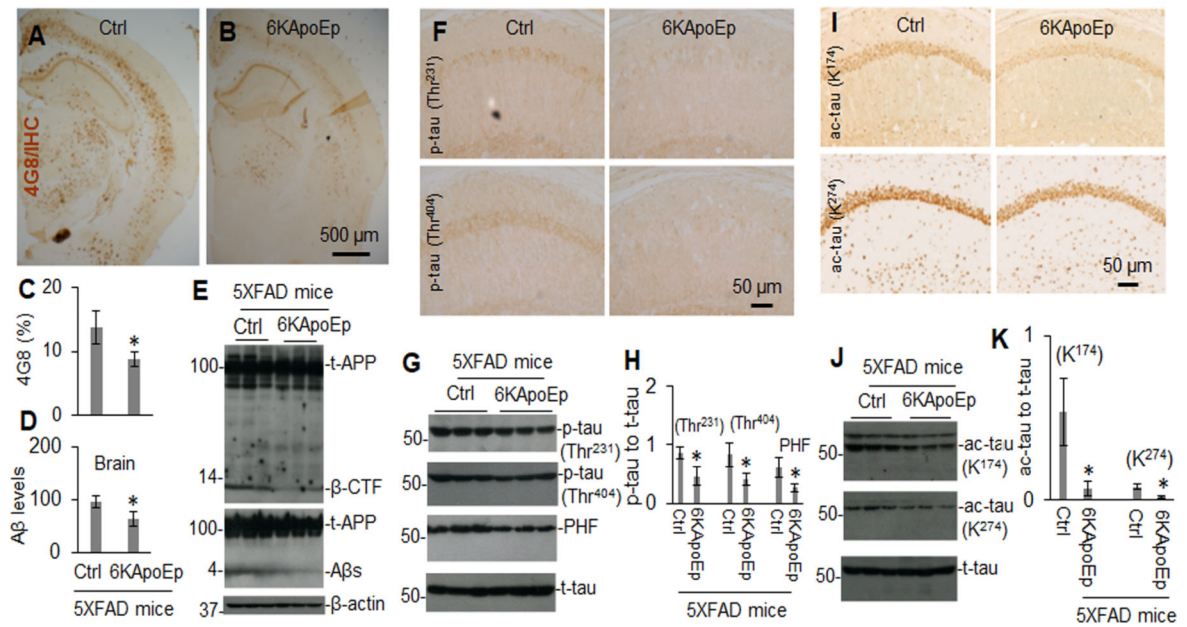
Figure 5. 6KApoEp inhibits APP trafficking to the cell surface and markedly mitigates p44/42 MAPK phosphorylation induced by apoE.

CHO/APPwt cells were treated with PBS control (Ctrl), 6KApoEp at 10 μM, apoE4 at 10 μg/mL, or 6KApoEp and apoE4, for 2 h followed by Aβ and sAPPα ELISA (**A, B**, *top panels*) and WB analysis using 82E1 or 2B3 antibody, respectively (**A, B**, *lower panels*). In addition, full-length APP (f-APP, short and long exp, exposure), α/β-CTF and total APP in cell lysates were also analyzed by WB using anti-C-terminal APP750/70 (pC-APP; **C**, *top panel*) and anti-N-terminal APP antibody (6E10; **c**, *lower panel*). Cell lysates were biotinylated and immunoprecipitated using Neutravidin beads and intracellular proteins obtained by Neutravidin depletion (intra) and cell surface proteins obtained by Neutravidin precipitation (cell surf) were analyzed for f-APP, LDLR, and LRP1 by WB using 6E10, anti-LDLR and anti-LRPl antibodies (**D**). Band density ratios of cell surf or intra to total f-APP was determined by densitometry analysis (**E**). Cellular membrane associated full-length APP was analyzed by flow cytometry and presented as the mean (± s.d.) median FL-1-A (**F**). Cultured cells were stained with mouse anti-N-terminal APP (22C11) and rabbit anti-C-terminal APP (pC-APP) primary antibodies after permeabilization (perm, 0.05% Triton X-100, 5 min) or directly (without perm) and observed using an Olympus FV1000 laser scanning confocal microscope (**G**). Alexa Fluor 594 donkey anti-rabbit and Alexa Fluor 488 goat anti-mouse IgG was used to detect APP. In addition, CHO/APPwt cells were treated with apoE4 at 10 μg/mL in the absence or presence of 6KApoEp at 10 μM, for 0 to 180 min followed by determination of total p44/42 (t-p44/42), t-p38 and phosphorylated-p44/p42 (pp44/42/), and pp38 MAPK levels in cell lysates by WB analysis (**H**). ELISA results are representative of three independent experiments with each condition triplicated and presented as the mean (± s.d.). Asterisk indicates $p < 0.05$ compared with Ctrl as determined by *t* test.

Figure 6. Peripheral administration of ApoEp significantly enhances β-amyloid- and tau-associated pathologies.

3XTg-AD mice (n = six mice, three female/three male) at 9 months of age were treated with ApoEp at 250 μg/kg or vehicle control (Ctrl, PBS alone) i.p. daily for 12 weeks. Following sacrifice, Aβ in brain coronal sections were analyzed by immunohistochemistry staining (IHC) using 4G8 antibody (**A, B**). Percentage of Aβ immunoreactive plaques from hippocampus and cortex was quantified by densitometry analysis (**C**). In addition, $Aβ_{1-40, 42}$ levels in brain homogenates were analyzed by ELISA (**D**) and total APP (t-APP), β-CTF and soluble total Aβ were determined by WB analysis using 6E10 (t-APP, β-CTF) and 82E1 (Aβs, **E**). Acetylated tau (ac-tau, K^{174} and K^{274}) and phosphorylated tau (p-tau, Thr^{231} and Thr^{181}) were determined by IHC (**D, I**) and WB analyses (**G, J**). Band density ratios of acetylated or phosphorylated tau to total tau was determined by densitometry analysis (**H, K**). Asterisk indicates $p < 0.05$ compared with vehicle control. ELISA results and band density ratios represented as the mean (± s.d.).

Figure 7. Peripheral administration of 6KApoEp markedly reduces β-amyloid and tau associated pathology.

5XFAD mice (n = ten mice, five female/five male) at 6 weeks of age were treated with 6KApoEp at 250 μg/kg or vehicle control (Ctrl, PBS alone) i.p. daily for 12 weeks followed by analysis of β-amyloid plaques in brain tissue coronal sections by IHC analysis using 4G8 (**A, B**, *top panels*). Percentage of Aβ immunoreactive plaques in hippocampus and cortex was quantified by densitometry analysis (**C**). In addition, Aβ$_{1-40, 42}$ levels in brain homogenates were analyzed by ELISA (**D**) and total APP (t-APP), β-CTF and soluble Aβ (Aβs) were determined in brain homogenates by WB analysis using 6E10 (t-APP, β-CTF) and 82E1 (t-APP, Aβs, **E**). Phosphorylated tau (p-tau, Thr^{231}, and Thr^{404}) and acetylated tau (ac-tau, K^{174}, and K^{274}) were also determined by IHC (**F, I**) and WB analyses (**G, J**) and band density ratios of acetylated or phosphorylated tau to total tau was determined by densitometry analysis (**H, K**). ELISA results and band density ratios represented as the mean (± s.d.). Asterisk indicates $p < 0.05$ versus Ctrl.
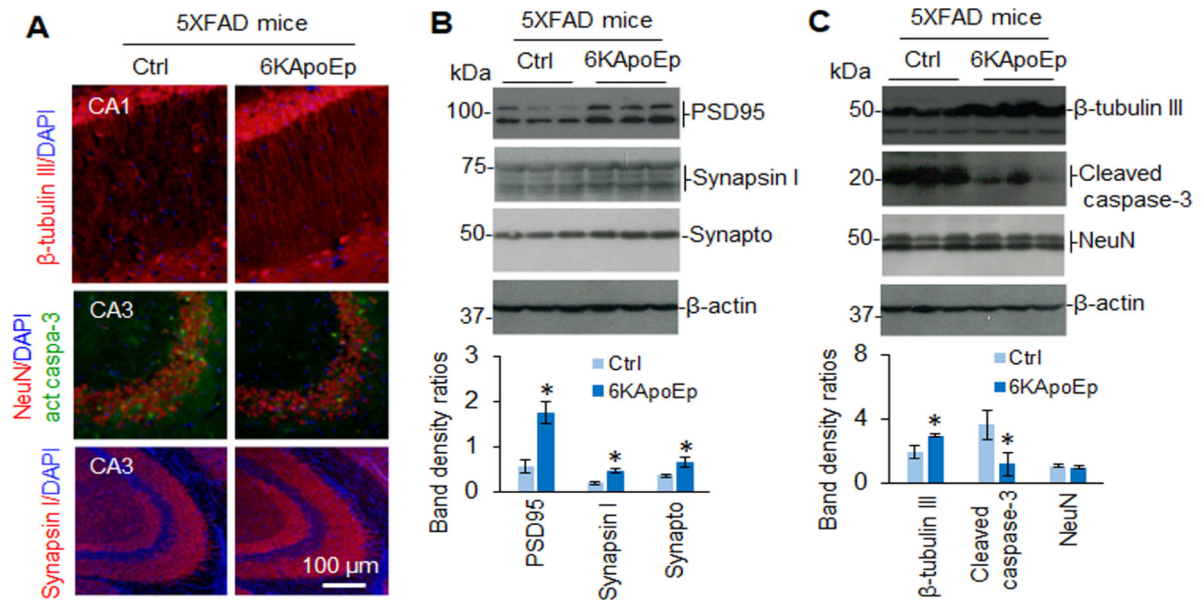
Figure 8. Peripheral administration of 6KApoEp significantly increases pre-synaptic snynaptophysin and post-synaptic PDS95 protein expression.

5XFAD mice (n = ten mice, five female/five male) at 6 weeks of age were treated with 6KApoEp at 250 µg/kg or vehicle control (Ctrl, PBS alone) i.p. daily for 12 weeks followed by analysis of neurogenesis in brain tissue coronal sections by IHC and IF. Neuronal (β-tubulin III, NeuN, and synapsin I), presynaptic snynaptophysin (synapto), post-synaptic PDS95, and apoptotic cleaved caspase-3 were determined in brain tissue coronal sections by IF staining **(A)** and in brain homogenates by WB analysis **(B, C**, *upper panels*). Band density ratios of each protein to β-actin was determined by densitometry analysis **(B, C**, *lower panes*). WB band density ratios represented as the mean (± s.d.). Asterisk indicates $p < 0.05$ versus Ctrl.
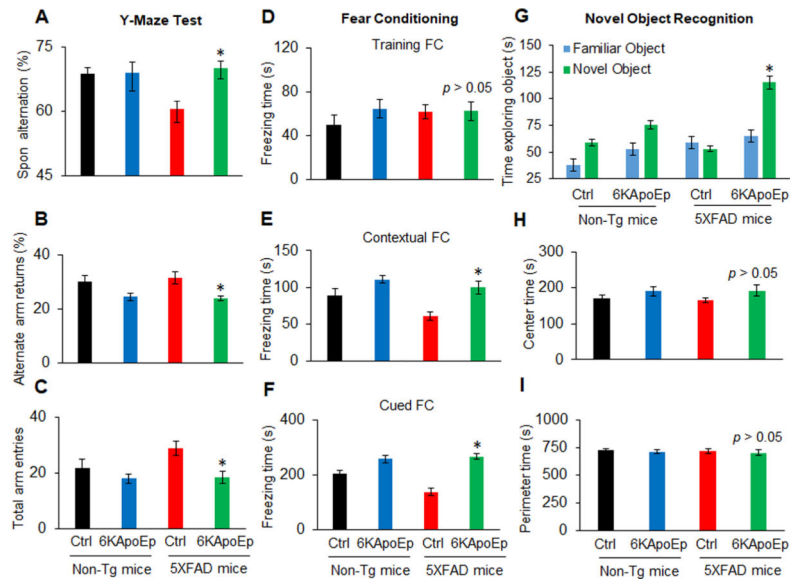
Figure 9. 6KApoEp treatment improves hippocampal-dependent learning and memory in 5XFAD mice.

Cognitive function and anxiety were determined after treatment of 5XFAD and non-transgenic control mice (n = ten mice, five female/five male) with 6KApoEp or vehicle PBS (Ctrl). Spontaneous (Spon) alternation, alternate arm returns and total arm entries were determined for the Y-maze testing (**A-C**). Total freezing times during the training and contextual and cued testing after training were determined for the fear condition testing (**D-F**). In addition, total times exploring familiar and novel objects were determined for the novel object recognition testing (**G**) and total times exploring central and peripheral zones were determined for the open field testing (**H, I**). 5XFAD mice exhibited impaired cognitive functioning as shown by reduced spontaneous alternation, freezing in the context and cued testing and ability to discriminate between novel and familiar objects compared with non-transgenic mice, which was reversed by 6KApoEp treatment. 5XFAD mice or treatment with 6KApoEp did not exhibit altered anxiety, as determined by time spent in center or perimeter of the open field test. Data are presented as the mean (± s.d.). Asterisk indicates $p < 0.05$ as determined by ANOVA.
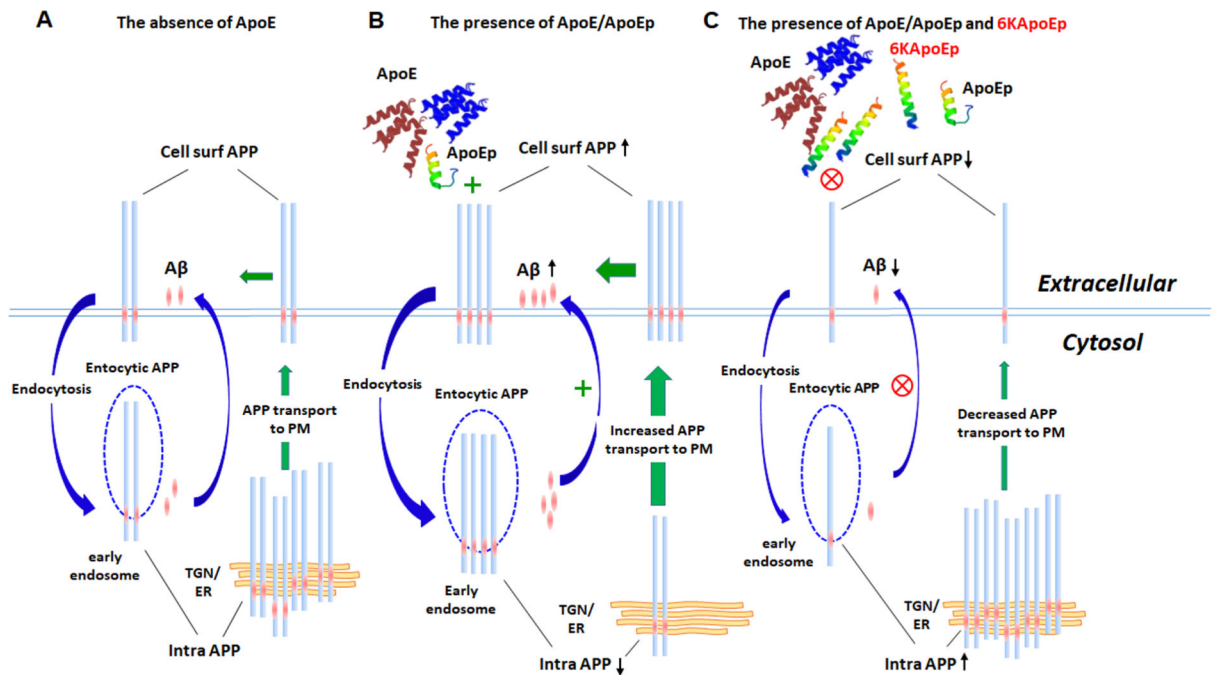
Figure 10. Schematic illustration of a novel apoE antagonist (6KApoEp) functionally blocking apoE or apoE LDLR binding domain peptide (ApoEp) interaction with N-terminal APP and inhibiting Aβ generation by reducing APP trafficking from trans-Golgi network and endoplasmic reticulum to the plasma membrane.

(**A**) Under physiological conditions, cell surface APP (Cell surf APP) auto internalizes into the cells *via* clathrin-mediated vesicles but β-site amyloid precursor protein cleaving enzyme 1 (BACE1) internalizes *via* ADP-ribosylation factor 6 (ARF-6) mediated endocytic pathway. APP β-cleavage occurs when lateral compartmentalization of APP and BACE1 meet in the early endosome at low pH and after additional γ-secretase cleavage generate Aβ, which can be secreted from the cell. In addition, newly synthesized APP travels through the secretory pathway from endoplasmic reticulum (ER) to the plasma membrane (PM) *via* the trans-Golgi network (TGN). (**B**) ApoE and/or apoE LDLR binding domain peptide (ApoEp) interaction with N-terminal APP increase Aβ generation by promoting internalization of APP *via* the endocytic pathway. In addition, binding of apoE and/or ApoEp with N-terminal APP markedly increases the trafficking of APP from ER and TGN to the plasma membrane, as evidenced by increased cell surface APP and decreased intracellular APP (Intra APP). (**c**) 6KApoEp inhibits apoE and/or ApoEp physical interaction with N-terminal APP, which decreases APP endocytosis and trafficking from ER and TGN to the plasma membrane, as evidenced by decreased cell surface and increased intracellular APP, reducing both sAPPα and Aβ generation.